Human Molecular Genetics, 2016, Vol. 25, No. 16 3476–3490

doi: 10.1093/hmg/ddw189
Advance Access Publication Date: 22 June 2016
Original Article

ORIGINAL ARTICLE

The PINK1, synphilin-1 and SIAH-1 complex constitutes a novel mitophagy pathway

Raymonde Szargel, Vered Shani, Fatimah Abd Elghani, Lucy N. Mekies, Esti Liani, Ruth Rott and Simone Engelender*

Department of Biochemistry, The B. Rappaport Faculty of Medicine and Institute of Medical Research, Technion-Israel Institute of Technology, Haifa 31096, Israel

*To whom correspondence should be addressed at: Tel: +972 48295416; Fax: +972 48295419; Email: simone@tx.technion.ac.il

Abstract

PTEN-induced putative kinase 1 (PINK1) and parkin are mutated in familial forms of Parkinson's disease and are important in promoting the mitophagy of damaged mitochondria. In this study, we showed that synphilin-1 interacted with PINK1 and was recruited to the mitochondria. Once in the mitochondria, it promoted PINK1-dependent mitophagy, as revealed by Atg5 knockdown experiments and the recruitment of LC3 and Lamp1 to the mitochondria. PINK1–synphilin-1 mitophagy did not depend on PINK1-mediated phosphorylation of synphilin-1 and occurred in the absence of parkin. Synphilin-1 itself caused depolarization of the mitochondria and increased the amount of uncleaved PINK1 at the organelle. Furthermore, synphilin-1 recruited seven in absentia homolog (SIAH)-1 to the mitochondria where it promoted mitochondrial protein ubiquitination and subsequent mitophagy. Mitophagy via this pathway was impaired by synphilin-1 knockdown or by the use of a synphilin-1 mutant that is unable to recruit SIAH-1 to the mitochondria. Likewise, knockdown of SIAH-1 or the use of a catalytically inactive SIAH-1 mutant abrogated mitophagy. PINK1 disease mutants failed to recruit synphilin-1 and did not activate mitophagy, indicating that PINK1–synphilin-1–SIAH-1 represents a new parkin-independent mitophagy pathway. Drugs that activate this pathway will provide a novel strategy to promote the clearance of damaged mitochondria in Parkinson's disease.

Introduction

Parkinson's disease (PD) is one of the most common neurodegenerative diseases, which leads to the degeneration of dopaminergic neurons in the substantia nigra and is associated with the presence of inclusion bodies, known as Lewy bodies (1,2). Mutations in α-synuclein cause familial PD (1,3), and α-synuclein is also a major component of Lewy bodies in sporadic forms of the disease (4), thus supporting its pathophysiological role in PD and other α-synucleinopathies. Additional genes are also implicated in both familial and sporadic PD. Mutations in parkin and PTEN-induced putative kinase 1 (PINK1) cause autosomal recessive forms of the disease (5,6), and together, these proteins play an important role in maintaining mitochondrial homeostasis (7,8).

We have previously shown that synphilin-1 interacts with α-synuclein *in vivo* and leads to the formation of inclusion bodies in cultured cells and mice (9–11). Synphilin-1 is enriched in the brain and is also present in Lewy bodies (12). It interacts with parkin, which ubiquitinates α-synuclein/synphilin-1 inclusions (13). Likewise, E3 ubiquitin-ligase seven in absentia homolog (SIAH)-1 and 2 interact with and ubiquitinate synphilin-1 (14,15). The inability of proteasomes to degrade ubiquitinated synphilin-1 leads to the formation of cytosolic synphilin-1/SIAH inclusions, which also contain α-synuclein (14). Synphilin-1 ameliorates α-synuclein pathology in double-transgenic mice,

Received: May 25, 2016. **Revised:** May 25, 2016. **Accepted:** June 14, 2016

thus indicating that it may have a neuroprotective role (10). However, its role in cell homeostasis has not been thoroughly investigated.

Macroautophagy (hereafter referred to as autophagy) is required for the degradation of dysfunctional organelles and inclusions of aggregated proteins (16). Similar to proteasomes, the autophagic pathway may be dysfunctional in PD (17), raising the possibility that inhibition of both proteasomal and autophagy pathways may cause protein accumulation and toxicity observed in the disease. Interestingly, synphilin-1 is also associated with autophagy, as it accelerates the autophagic degradation of α-synuclein-containing inclusions (18). In addition, the levels of autophagy-related proteins are increased in synphilin-1 transgenic mice, and synphilin-1 is directly targeted to the autophagic pathway in cultured cells (10,11,19).

PINK1 is a mitochondrial protein that is recruited and retained at the mitochondrial outer membrane upon mitochondrial depolarization, leading to the translocation of parkin to the organelle (20–25). Once at the mitochondria, parkin ubiquitinates outer membrane proteins, leading to the recruitment of autophagic proteins, and subsequently mitophagy (23,26). This process is amplified by PINK1-mediated phosphorylation of ubiquitin that activates parkin (27–29). Disease mutations of PINK1 and parkin have deleterious effects on mitophagy in cell models (21,22,24,25,30), suggesting that the accumulation of dysfunctional mitochondria may play a role in PD. Accordingly, α-synuclein transgenic mice and PD patients show evidence of accumulation of dysfunctional brain mitochondria (31).

Because mitophagy represents an important process in the maintenance of mitochondrial health (32,33), it is conceivable that other pathways are also activated, in addition to the PINK1–parkin pathway. Indeed, Drp1 promotes mitochondrial degradation, independent of PINK1–parkin (34). In another example, ambra1 promotes PINK1–parkin-dependent and PINK1–parkin-independent, mitophagy (35,36).

In this study, we show evidence supporting a new mitophagy pathway involving PINK1, synphilin-1 and SIAH-1. We found that synphilin-1 interacted with PINK1 *in vivo* and promoted its translocation to the mitochondria. It also promoted mitochondrial depolarization and increased the levels of uncleaved PINK1 at the organelle, leading to mitophagy. Furthermore, synphilin-1 recruited SIAH-1 to the mitochondria where it facilitated mitophagy. Recruitment of synphilin-1 to the mitochondria and subsequent mitophagy was defective in PINK1 disease mutations, indicating that the PINK1–synphilin-1–SIAH-1 pathway may represent an important mitochondrial degradation pathway in PD.

Results

Synphilin-1 was previously reported to interact with PINK1 in yeast by the two-hybrid system (37), but there has been no biochemical demonstration of this interaction, and the role of a putative PINK1–synphilin-1 complex remains unclear. In our study, we investigated this interaction by performing transfection experiments in dopaminergic SH-SY5Y cells. We found that synphilin-1 co-immunoprecipitated with PINK1 (Fig. 1A), indicating that these proteins interact in mammalian cells. Co-immunoprecipitation using different regions of synphilin-1 showed that amino acids 350–549 of synphilin-1, and to a lesser extent amino acids 550–769, mediated the interaction with PINK1 (Fig. 1B). These two regions encompass the ankyrin-like repeats of synphilin-1 (9), suggesting that the ankyrin-like repeats may play a role in mediating its interaction with PINK1. Moreover, synphilin-1 co-immunoprecipitated with PINK1 from rat brain homogenates, but not with control immunoglobulin G (IgG) (Fig. 1C), indicating that synphilin-1 interacts with PINK1 *in vivo*. The relatively lower size of synphilin-1 in the brain is compatible with its processing during neuronal maturation (9,38).

As previously reported (6), PINK1 is associated with the mitochondria (Fig. 2A). Likewise, we found that ectopically expressed synphilin-1 is also associated with mitochondria (Fig. 2B), and this interaction was resistant to high salt and detergent extraction, indicating a strong interaction (Fig. 2C). Endogenous synphilin-1 from rat brain cortex was present in the mitochondrial fraction and was resistant to detergent extraction as well (Fig. 2D), indicating that the association of synphilin-1 with mitochondria is strong and occurs *in vivo*.

Although PINK1 expression decreased the steady-state levels of synphilin-1 (Fig. 3A), this was associated with increased translocation of ectopically expressed synphilin-1 from the cytosol to the mitochondria (Fig. 3B). In addition, PINK1 also promoted higher accumulation of endogenous synphilin-1 to the mitochondrial fraction (Fig. 3C). Immunocytochemistry confirmed the PINK1-mediated accumulation of synphilin-1 in the mitochondria where synphilin-1 co-localized with GFP-mito (green fluorescent protein fused to cytochrome *c* oxidase subunit VIII mitochondrial targeting sequence) (Fig. 3D and E). Mutations of PINK1 at the catalytic site (K219M; KD) (21) did not alter its ability to recruit synphilin-1 to the mitochondria (Fig. 3E), indicating that the translocation of synphilin-1 is nevertheless independent of PINK1 kinase activity.

Additional evidence that synphilin-1 translocation depends on PINK1 comes from PINK1 knockdown experiments using short interfering RNA (siRNA), which resulted in a 50% decrease in synphilin-1 levels at the mitochondria (Fig. 3F), along with approximately 80% decrease in endogenous PINK1 (Fig. 3G).

Because synphilin-1 is a parkin substrate (13,39), we explored a possible association between the PINK1–parkin pathway and synphilin-1 translocation. While parkin robustly translocated to the mitochondria in the presence of PINK1 (Fig. 3D and H), its knockdown or overexpression did not change the ability of PINK1 to promote the translocation of synphilin-1 to the mitochondria (Fig. 3I and K). A knockdown of approximately 85% was obtained with the use siRNA to parkin (Fig. 3J). Conversely, synphilin-1 expression did not affect the mitochondrial translocation of parkin (Fig. 3L), suggesting that parkin and synphilin-1 binding at the mitochondria occurs independently of each other.

In order to determine the role of synphilin-1 in mitophagy, we estimated the mitochondrial content by immunocytochemistry experiments for the outer mitochondrial membrane protein Tom20 and the matrix mitochondrial protein HSP60. Synphilin-1 potentiated the PINK1-mediated reduction in mitochondrial content, compatible with increased mitophagy (Fig. 4A–D).

Increased mitophagy promoted by synphilin-1 was dependent on PINK1, as synphilin-1 alone was unable to significantly increase mitophagy levels (Fig. 4B and D). The same is true for PINK1 alone, as mitophagy levels were lower in the absence of synphilin-1 (Fig. 4B and D). Therefore, these data are in agreement with the notion that synphilin-1 and PINK1 act in concert at the mitochondria to increase mitophagy.

As seen in the synphilin-1 translocation process, PINK1 KD catalytically inactive mutant had the same effect as the PINK1 wild-type in synphilin-1-mediated mitophagy (Fig. 4A–D). Therefore, the observed mitophagy by PINK1–synphilin-1 does

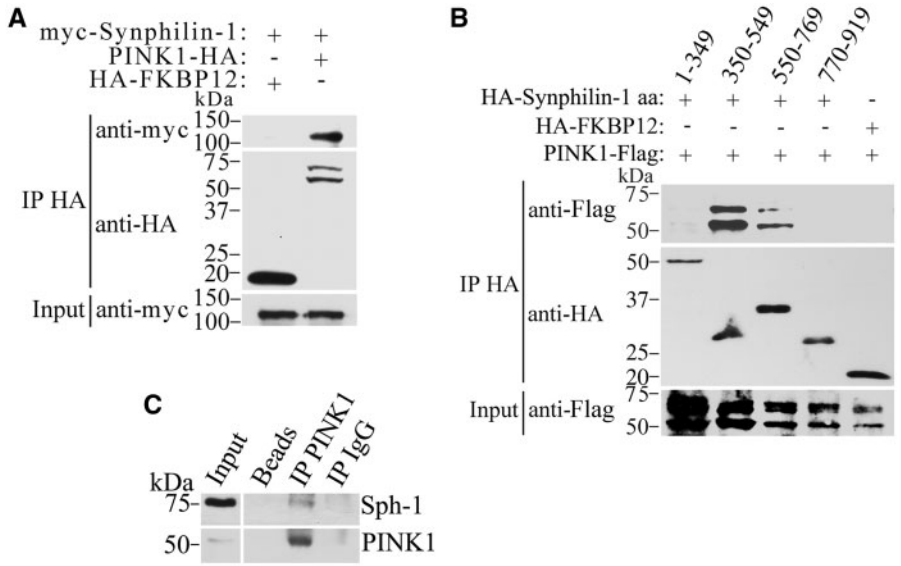

Figure 1. Synphilin-1 interacts with PINK1. (**A**) Human dopaminergic SH-SY5Y cells were co-transfected with myc-synphilin-1, in the presence of PINK1-HA or the control HA-FKBP12. HA-tagged proteins were immunoprecipitated using anti-HA antibody (middle), and co-immunoprecipitation of myc-synphilin-1 was detected with anti-myc antibody (top). (**B**) SH-SY5Y cells were transfected with PINK1-Flag, in the presence of different HA-synphilin-1 constructs or HA-FKBP12. Co-immunoprecipitation of PINK1-Flag was detected using anti-Flag antibody (top). Immunoprecipitation of HA-tagged proteins was detected with anti-HA antibody (middle). (**C**) Endogenous PINK1 was immunoprecipitated from rat total brain lysate using anti-PINK1 antibody, and co-immunoprecipitation was revealed with anti-synphilin-1 antibody. Co-immunoprecipitation of synphilin-1 was not observed in the control coupled to IgG. Experiments are representative of three (A and B) and four (C) independent experiments.

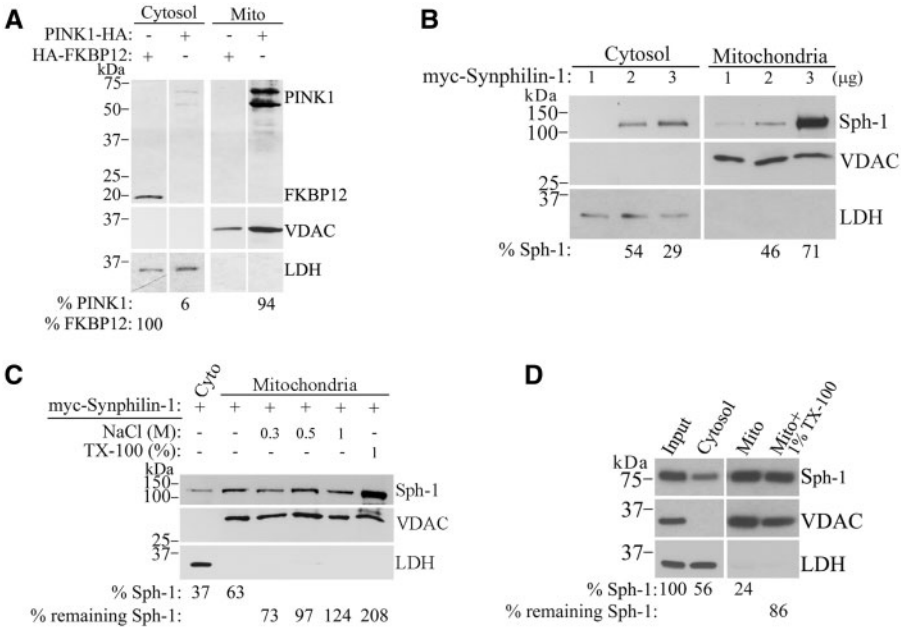

Figure 2. Synphilin-1 associates with mitochondria. (**A**) SH-SY5Y cells were transfected with 2 μg PINK1-HA or the control HA-FKBP12. Lysates were processed into cytosolic and mitochondrial fractions. Equal amounts of cytosolic and mitochondrial fractions were analyzed by western blotting. HA-tagged proteins were detected with anti-HA antibody (top). The percent of PINK1 and FKBP12 in cytosolic and mitochondrial fractions relative to their total protein levels is indicated at the bottom of the figure. (**B**) SH-SY5Y cells were transfected with increasing amounts of myc-synphilin-1, and lysates were processed into cytosolic and mitochondrial fractions. Myc-synphilin-1 was detected with anti-myc antibody (top). The percent of synphilin-1 in cytosolic and mitochondrial fractions relative to their total protein levels is indicated. (**C**) SH-SY5Y cells were transfected with myc-synphilin-1. After purification, mitochondrial fractions were washed under different stringencies. Myc-synphilin-1 was detected with anti-myc antibody (top). The percent of synphilin-1 in cytosolic and mitochondrial fractions relative to their total protein levels is indicated. The percent of remaining synphilin-1 in mitochondrial fractions after salt and detergent treatments is also indicated. (**D**) Rat brain cerebral cortices were homogenized and processed into cytosolic and mitochondrial fractions. Synphilin-1 was detected with anti-synphilin-1 antibody (top). The strength of the synphilin-1 interaction with brain mitochondria was tested by extracting mitochondrial fractions with 1% TX-100. The percent of synphilin-1 in cytosolic and mitochondrial fractions relative to its total protein level is indicated. The percent of remaining synphilin-1 in mitochondrial fraction after detergent treatment is also indicated. The purity of all cytosolic and mitochondria fractions was examined using anti-lactate dehydrogenase (LDH) and anti-voltage-dependent anion channel (VDAC) antibodies, respectively. All experiments are representative of at least three independent experiments.

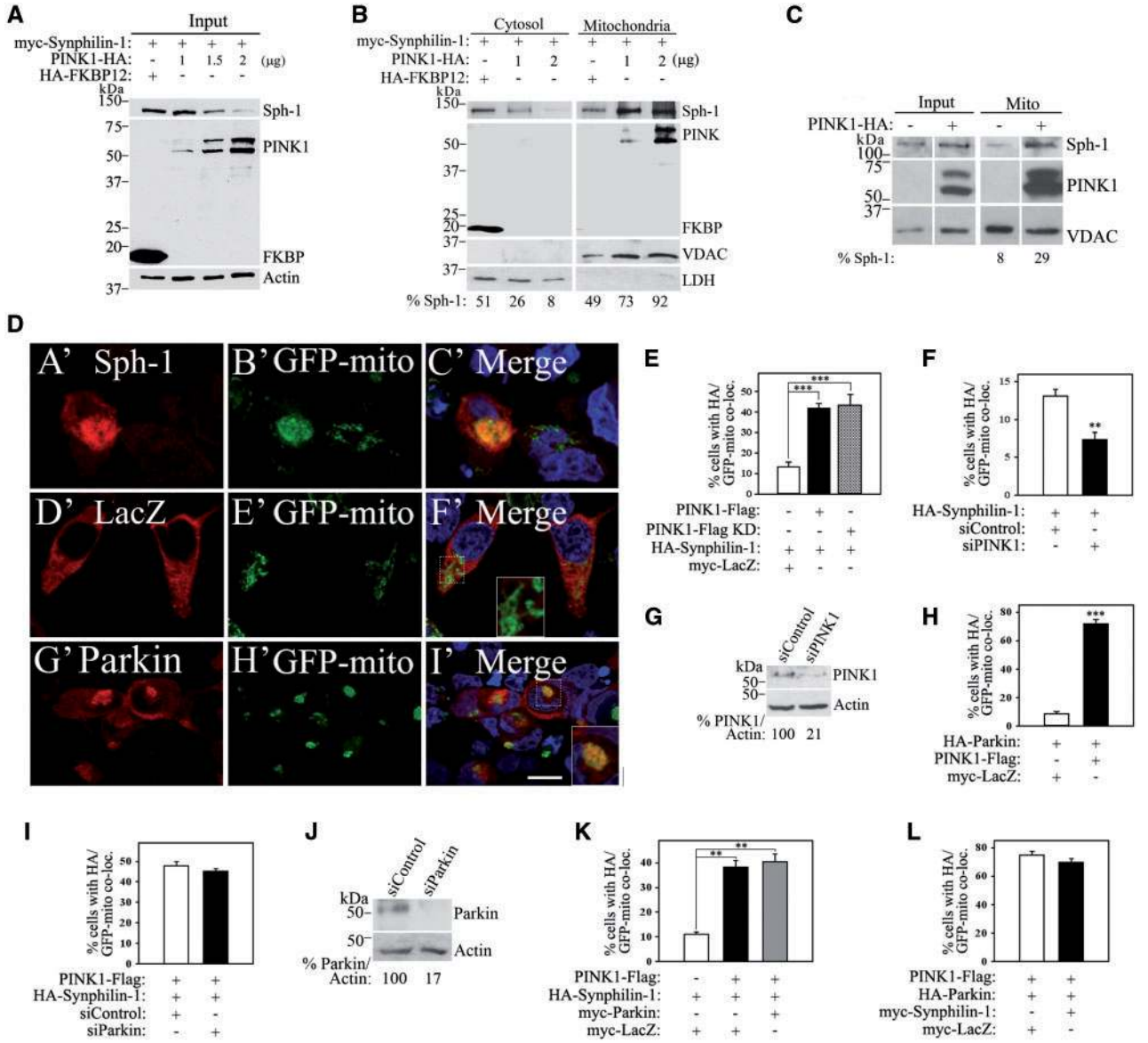

Figure 3. PINK1 increases mitochondrial translocation of synphilin-1. (**A**) SH-SY5Y cells were transfected with myc-synphilin-1, PINK1-HA or the control HA-FKBP12. The levels of synphilin-1 and PINK1 were monitored with anti-myc and anti-HA antibodies, respectively. Loading control was determined with anti-actin antibody. (**B**) SH-SY5Y cells were co-transfected with myc-synphilin-1, in the presence of the control HA-FKBP12 or PINK1-HA. Lysates were fractionated into cytosolic and mitochondrial fractions and were analyzed by western blotting. Myc-synphilin-1 was detected using anti-myc antibody (top) and PINK1-HA using anti-HA antibody (middle). The purity of cytosolic and mitochondrial fractions was examined using anti-lactate dehydrogenase (LDH) and anti-voltage-dependent anion channel (VDAC) antibodies, respectively. The percent of synphilin-1 in cytosolic and mitochondrial fractions relative to their total protein levels is indicated at the bottom of the figure. (**C**) SH-SY5Y cells were transfected with and without 2 μg PINK1-HA. Lysates were fractionated into mitochondrial fractions and were analyzed by western blotting. Endogenous synphilin-1 was detected using anti-synphilin-1 antibody (top) and PINK1-HA using anti-HA antibody (middle). The enrichment of mitochondrial fractions was examined using anti-VDAC antibody. The percent of synphilin-1 in mitochondrial fractions relative to their total protein levels is indicated. (**D**) SH-SY5Y cells were transfected with PINK1-Flag and green fluorescent protein-mito (GFP-mito), in the presence of myc-synphilin-1, myc-parkin or myc-LacZ. Cells were processed for immunocytochemistry, and co-localization of myc-proteins with GFP-mito was determined by confocal microscopy. Insets represent increased magnification of selected areas within cells. (**E**) SH-SY5Y cells were transfected with or without PINK1-Flag (wild-type or kinase-deficient K219M; KD), in the presence of HA-synphilin-1 and GFP-mito. Cells were processed for immunocytochemistry, and co-localization of HA-synphilin-1 with GFP-mito was determined by confocal microscopy. The graph represents the percentage of HA-synphilin-1 co-localization with mitochondria (GFP-mito). (**F**) SH-SY5Y cells were transfected with HA-synphilin-1, in the presence of siRNA control or siRNA to PINK1. Cells were processed and analyzed as in (E). (**G**) SH-SY5Y cells were transfected with siRNA to PINK1 or siRNA control. PINK1 levels in total cell lysates were detected using anti-PINK1 antibody (top). Loading control was monitored with anti-actin antibody (bottom). The percentage of PINK1 present in cell lysates relative to actin levels is shown at the bottom of the figure. (**H**) SH-SY5Y cells were transfected with HA-parkin, in the absence or presence of PINK1-Flag, and the mitochondrial marker GFP-mito. Cells were processed as in (E), and co-localization of HA-parkin with GFP-mito was determined by confocal microscopy. The graph represents the percentage of HA-parkin co-localization with mitochondria (GFP-mito). (**I**) SH-SY cells were transfected with PINK1-Flag and HA-synphilin-1, in the presence of siRNA control or siRNA to parkin. Cells were processed and analyzed as in (E). (**J**) SH-SY5Y cells were transfected with siRNA to parkin or siRNA control. The presence of parkin in total cell lysates was detected using anti-parkin antibody (top). The percentage of parkin present in cell lysates relative to actin levels is shown at the bottom of the figure. (**K**) SH-SY5Y cells were transfected with HA-synphilin-1, with or without PINK1-Flag, in the presence of myc-parkin or myc-LacZ. Localization of synphilin-1 was analyzed as in (E). (**L**) SH-SY5Y cells were transfected with PINK1-Flag and HA-parkin, in the presence of myc-synphilin-1 or myc-LacZ. Co-localization of parkin was analyzed as in (H). Experiments are representative of at least three independent experiments (A–D, G and J). Values represent the average ± S.E.M. of four (E) or three experiments (F, H, I, K, L). ** and ***Different from control at $P < 0.01$ and $P = 0.001$, respectively (Student's *t*-test). Scale bar, 25 μm.

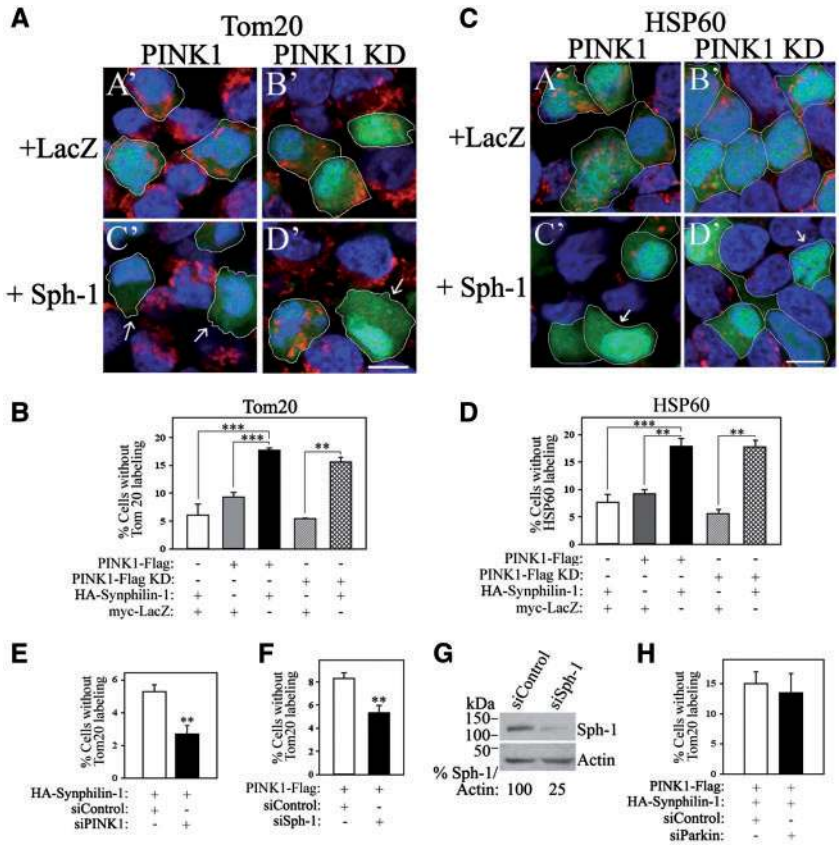

Figure 4. Synphilin-1 promotes PINK1-dependent mitophagy. (**A**) SH-SY5Y cells were transfected with PINK1-Flag (wild-type or KD), green fluorescent protein (GFP; as marker for transfection), in the presence of HA-synphilin-1 or myc-LacZ. Cells were processed for immunocytochemistry using anti-Tom20 antibody as a marker for mitochondria (in red). Mitophagy was determined by the presence of Tom20 labeling in GFP-positive cells. Cells transfected with GFP-mito are outlined to enable proper visualization, and cells devoid of Tom20 labeling are indicated by arrows. (**B**) SH-SY5Y cells were transfected and analyzed as in (A). The graph represents the percentage of transfected cells without Tom20 labeling. (**C**) SH-SY5Y cells were transfected as in (A), and immunocytochemistry was performed using anti-HSP60 antibody as an internal mitochondrial marker (in red). Cells transfected with GFP-mito are outlined and cells devoid of HSP60 labeling are indicated by arrows. **D,** SH-SY5Y cells were transfected as in (A) and analyzed by immunocytochemistry using anti-HSP60 antibody as in (C). The graph represents the percentage of transfected cells without HSP60 labeling. (**E**) SH-SY cells were transfected with HA-synphilin-1, in the presence of siRNA control or siRNA to PINK1. Cells were processed and analyzed as in (A). The graph represents the percentage of transfected cells without Tom20 labeling. (**F**) SH-SY cells were transfected with PINK1-Flag, in the presence of siRNA control or siRNA to synphilin-1. Cells were processed and analyzed as in (A). The graph represents the percentage of transfected cells without Tom20 labeling. (**G**) SH-SY5Y cells were transfected with siRNA to synphilin-1 or siRNA control. The presence of synphilin-1 in total cell lysates was detected using anti-synphilin-1 antibody (top). The percentage of synphilin-1 present in cell lysates relative to actin levels is shown at the bottom of the figure. (**H**) SH-SY5Y cells were transfected with PINK1-Flag and HA-synphilin-1, in the presence of siRNA control or siRNA to parkin. Cells were processed and analyzed as in (A). The graph represents the percentage of transfected cells without Tom20 labeling. Experiments are representative of five (A and C) and three (G) independent experiments. Values represent the average ± S.E.M. of five (B and D) or four experiments (E, F and H). ** and***Different from control at $P < 0.01$ and $P = 0.001$, respectively (Student's *t*-test). Scale bar, 25 μm.

not require ubiquitin phosphorylation by PINK1 and subsequent activation of parkin (27–29).

As additional control, knockdown of endogenous PINK1 by siRNA (Fig. 3G) led to a 50% decrease in the levels of synphilin-1-dependent mitophagy (Fig. 4E). siRNA-mediated synphilin-1 knockdown resulted in a 40% decrease in the levels of PINK1-dependent mitophagy (Fig. 4F), along with a 75% decrease in endogenous synphilin-1 levels (Fig. 4G). Moreover, knockdown of endogenous parkin (Fig. 3J) did not interfere with the mitophagy promoted by PINK1–synphilin-1 (Fig. 4H). These findings are consistent with the notion that PINK1–synphilin-1-mediated mitophagy does not require parkin.

Next, we analyzed autophagosome formation by determining the association between LC3 and mitochondria. We found that co-expression of PINK1 and synphilin-1 increased by 3-fold the amount of LC3 large puncta at the proximity of the mitochondria, compared to PINK1 or synphilin-1 alone (Fig. 5A and B). In addition, we investigated if autophagosome formation promoted by PINK1–synphilin-1 led to lysosomal degradation of mitochondrial content by determining the association between the lysosomal marker Lamp1 and mitochondria. Synphilin-1 and PINK1 tripled the amount of Lamp1 large puncta that was in proximity to the mitochondria, compared to that obtained with synphilin-1 or PINK1 alone (Fig. 5C and D).

Autophagy-related inhibitors, such as 3-MA and chloroquine, abolished PINK1–synphilin-1-dependent mitophagy (Fig. 5E). Mitophagy by PINK1–synphilin-1 decreased by 50% upon knockdown (approximately 60%) of the autophagy component Atg5 (40) (Fig. 5F and G). On the other hand, the proteasome inhibitor lactacystin did not inhibit mitophagy (Fig. 5E),

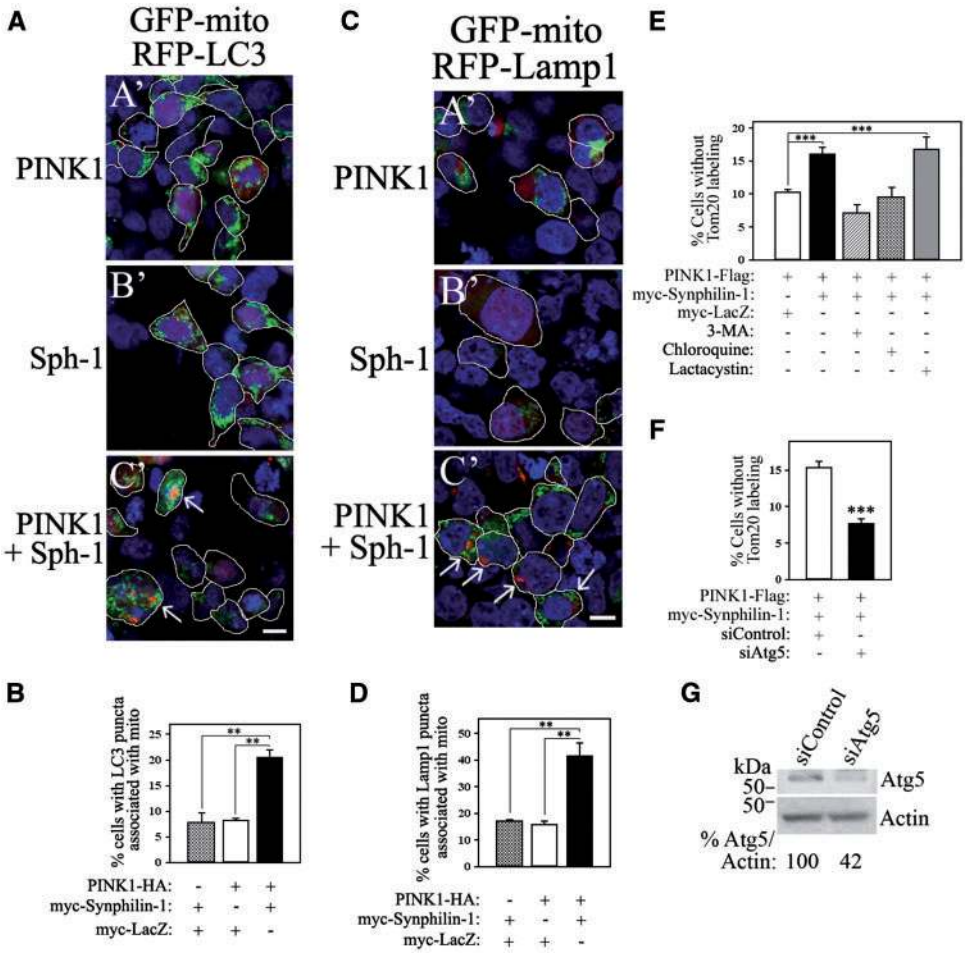

Figure 5. Translocation of synphilin-1 to the mitochondria recruits components of the autophagy pathway. (**A**) SH-SY5Y cells were transfected with green fluorescent protein-mito (GFP-mito) and RFP-LC3, in the presence of PINK1-HA, myc-synphilin-1 or myc-LacZ. Association of RFP-LC3 large puncta with GFP-mito was determined by confocal microscopy. Cells transfected with GFP-mito and RFP-LC3 are outlined and cells containing large LC3 puncta closely associated with the mitochondria are indicated by arrows. (**B**) Cells were transfected and analyzed as in (A). The graph represents the percentage of cells that exhibit large RFP-LC3 puncta in close association with mitochondria (GFP-mito). (**C**) SH-SY5Y cells were transfected with GFP-mito, RFP-Lamp1 and PINK1-HA, in the presence of myc-synphilin-1 or myc-LacZ. The close association of large RFP-Lamp1 puncta with GFP-mito was determined by confocal microscopy. Cells transfected with GFP-mito and RFP-Lamp1 are outlined and cells containing large Lamp1 puncta closely associated with the mitochondria are indicated by arrows. (**D**) Cells were transfected as indicated and analyzed as in (C). The graph represents the percentage of cells that exhibit large RFP-Lamp1 puncta closely associated with the mitochondria (GFP-mito). (**E**) SH-SY5Y cells were transfected with PINK1-Flag and GFP, in the presence of myc-synphilin-1 or myc-LacZ. Cells were treated with 10 mM 3-MA, 30 μM chloroquine, 10 μM lactacystin or DMSO for 16 h. The presence of Tom20 in GFP-positive cells was determined by immunocytochemistry and analyzed by confocal microscopy. The graph represents the percentage of transfected cells without Tom20 labeling. (**F**) SH-SY5Y cells were transfected with PINK1-Flag, myc-synphilin-1 and GFP, in the presence of siRNA control or siRNA to Atg5. Cells were processed for immunocytochemistry and confocal microscopy using anti-Tom20 antibody. The graph represents the percentage of transfected cells without Tom20 labeling. (**G**) SH-SY5Y cells were transfected with siRNA to Atg5 or siRNA control. Levels of Atg5 in total cell lysates were detected using anti-Atg5 antibody (top). The percentage of Atg5 present in cell lysates relative to actin levels are shown at the bottom of the figure. Experiments are representative of four (A and C) and three (G) independent experiments. Values represent the average ± S.E.M. of four (B and D) or five experiments (E and F). ** and ***Different from control at $P < 0.01$ and $P = 0.001$, respectively (Student's *t*-test). Scale bar, 25 μm.

suggesting that proteasomal degradation of synphilin-1 or outer membrane mitochondrial proteins are not required during PINK1–synphilin-1-mediated mitophagy.

Synphilin-1 promoted PINK1-dependent mitophagy in HeLa, HEK293 and SH-SY5Y cells (Fig. 6A–C and F), supporting a role for the PINK1–synphilin-1 pathway in additional mammalian cells. Because PINK1–parkin has been extensively studied in HeLa cells (22,24), we further compared the two pathways using this cell line. The PINK1–parkin pathway differs from that of PINK1–synphilin-1 in its requirement for an exogenous depolarizing agent. While mitophagy by PINK1–parkin pathway was observed only when mitochondria was depolarized by CCCP (Fig. 6D and E) (22,24), CCCP had no effect on mitophagy by PINK1–synphilin-1 in HeLa cells (Fig. 6D and E). The same was observed in SH-SY5Y cells, where depolarization increased mitophagy by PINK1–parkin pathway, but not by PINK1–synphilin-1 (Fig. 6F).

Next, we addressed the question of how PINK1–synphilin-1 causes mitophagy in the absence of an exogenous depolarizing agent. We found that synphilin-1 itself caused mitochondrial depolarization, as measured by the membrane potential indicator JC-1 (Fig. 7A and B). In support of these data, the ratio of uncleaved PINK1 relative to total PINK1 levels was increased in the presence of synphilin-1 (Fig. 7C). Most importantly, this was also observed with endogenous PINK1 (Fig. 7D). Together, the data suggest that synphilin-1 stabilizes uncleaved PINK1 at the

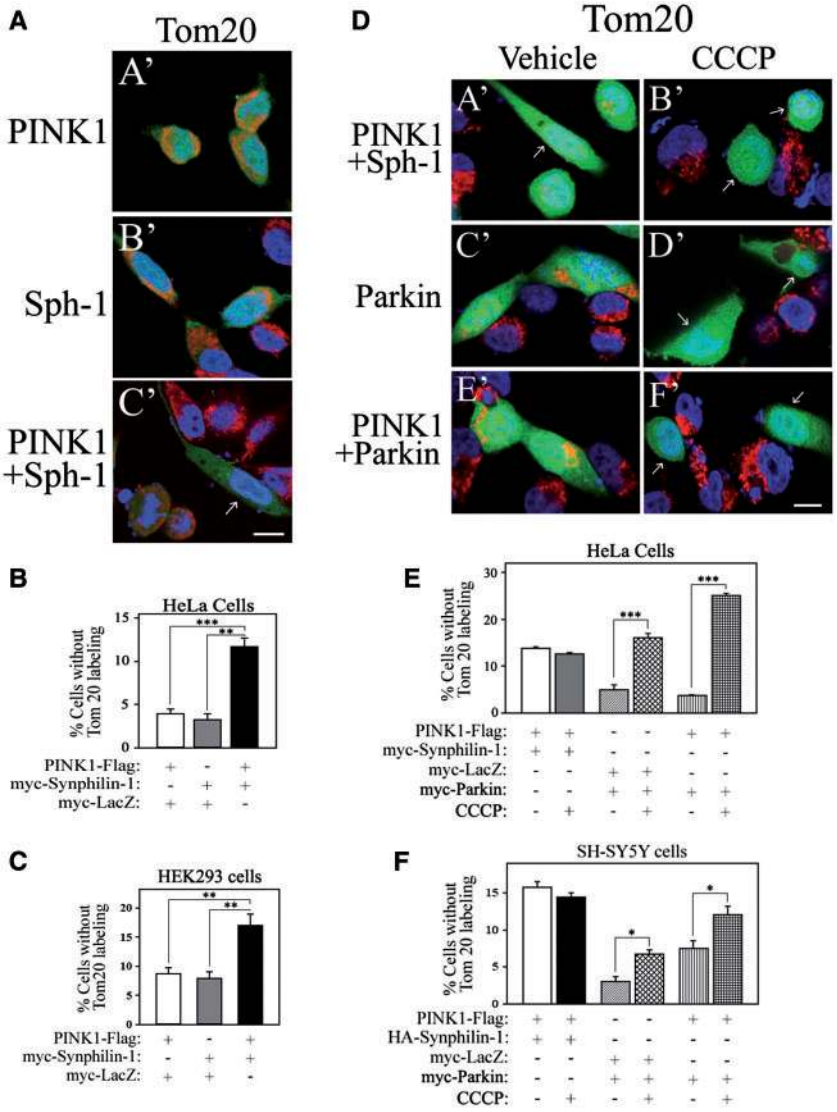

Figure 6. The PINK1–synphilin-1 pathway promotes mitophagy in different types of cells. (**A**) HeLa cells were transfected with green fluorescent protein (GFP) and different combinations of PINK1-Flag and myc-synphilin-1. Mitophagy was determined by the absence of Tom20 labeling in GFP-positive cells. Cells devoid of Tom20 labeling are indicated by arrows. (**B**) HeLa cells were transfected and analyzed as in (A). The graph represents the percentage of transfected cells without Tom20 labeling. (**C**) HEK293 cells were transfected and analyzed as in (A). The graph represents the percentage of transfected cells without Tom20 labeling. (**D**) HeLa cells were transfected with GFP and different combinations of PINK1-Flag, myc-synphilin-1 and myc-parkin. When indicated, 10 μM CCCP was added to the cells for 16 h. Mitophagy was determined by the absence of Tom20 labeling in GFP-positive cells. Cells devoid of Tom20 labeling are indicated by arrows. (**E**) HeLa cells were transfected and treated as in (D). The graph represents the percentage of transfected cells without Tom20 labeling. (**F**) SH-SY5Y cells were transfected and treated as in (D). The graph represents the percentage of transfected cells without Tom20 labeling. Experiments are representative of five independent experiments (A and D). Values represent the average ± S.E.M. of five (B and E) or four experiments (C and F). *, ** and ***Different from control at $P < 0.05$, $P = 0.01$ and $P = 0.001$, respectively (Student's *t*-test). Scale bar, 25 μm.

surface of the mitochondria, similar to the stabilization of uncleaved PINK1 levels promoted by CCCP treatment (22,24). Nevertheless, the stabilization of PINK1 by synphilin-1 at the mitochondria did not result in phosphorylation of synphilin-1, even under depolarization conditions (Fig. 7E), which is in agreement of the lack of effect of catalytically inactive PINK1 KD on PINK1–synphilin-1 mitophagy (Fig. 4A–D).

Ubiquitination of mitochondrial proteins by parkin is thought to be essential for mitophagy (24). We assessed whether an additional E3 ubiquitin-ligase mediates mitochondrial ubiquitination in the PINK1–synphilin-1 pathway. Because synphilin-1 interacts with SIAH-1 E3 ubiquitin-ligase (14,15), we investigated a possible role for SIAH in mediating mitochondrial ubiquitination. We found that only a small amount of SIAH-1 was located at the mitochondria in the presence of PINK1 alone (Fig. 8A–C); however, the co-expression of PINK1 and synphilin-1 significantly increased the levels of SIAH-1 at the mitochondria (Fig. 8A–C). The catalytically inactive SIAH-1 mutant (SIAH-1 DN) did not co-localize with the mitochondria in the presence of synphilin-1 and PINK1 (Fig. 8A-C), suggesting that the catalytic activity of SIAH-1 is required for its mitochondrial localization.

We next investigated the ubiquitination levels of mitochondrial proteins when the PINK1–synphilin-1–SIAH-1 pathway was activated. Western blot analysis revealed substantial mitochondrial ubiquitination in the presence of SIAH-1 but significantly less with SIAH-1 DN (Fig. 8C, bottom). Immunocytochemistry experiments confirmed that the

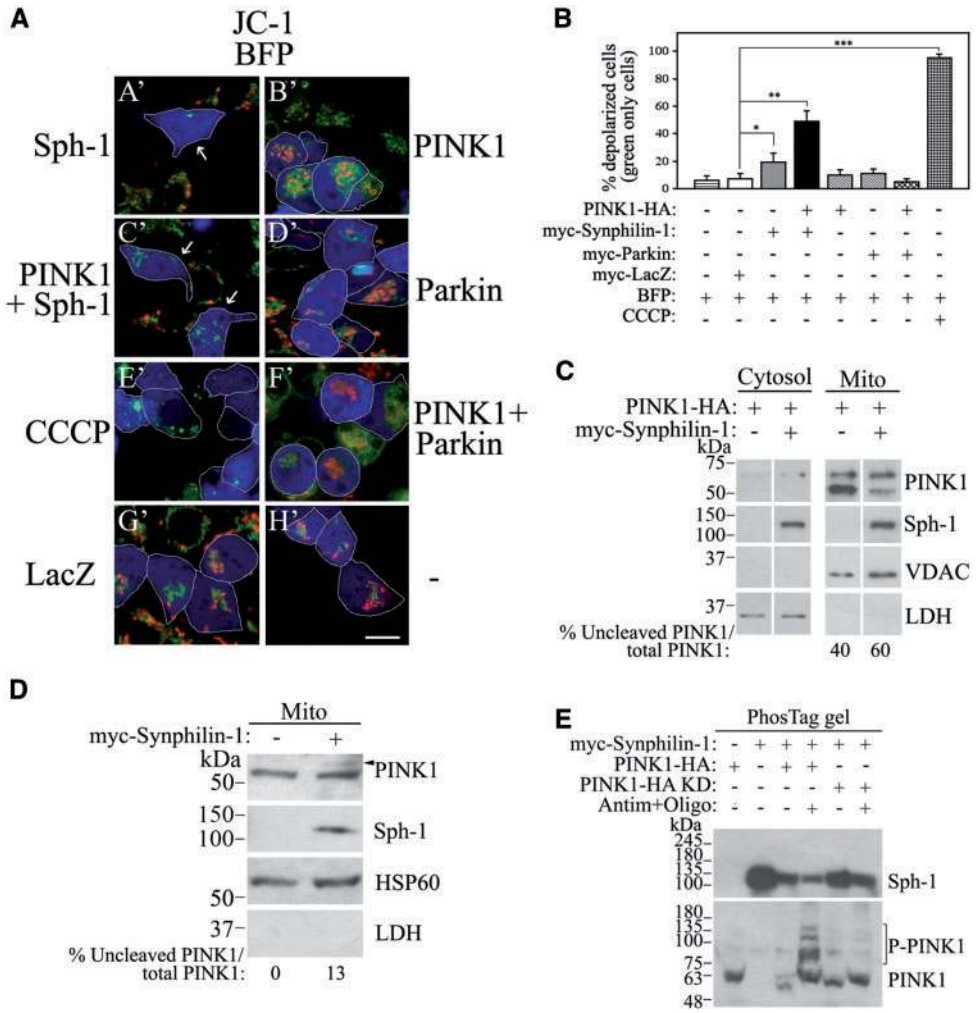

Figure 7. Synphilin-1 depolarizes mitochondria and stabilizes uncleaved PINK1. (**A**) SH-SY5Y cells were transfected with blue fluorescent protein (BFP; as a transfection marker), PINK1-HA, myc-synphilin-1, myc-parkin or myc-LacZ. Cells were incubated with JC-1 and analyzed by live microscopy. The presence of red JC-1 represents cells with polarized mitochondria, whereas the presence of green JC-1 represents cells with depolarized mitochondria (arrows). Transfected cells are outlined and cells with green only JC-1 (depolarized) are indicated by arrows. (**B**) SH-SY5Y cells were transfected and analyzed as in (A). The graph represents the percentage of transfected cells with depolarized mitochondria (with green only JC-1). (**C**) SH-SY5Y cells were transfected with 2 μg PINK1-HA, in the absence or presence of myc-synphilin-1. Lysates were processed into cytosolic and mitochondrial fractions and analyzed by western blot. PINK1 was detected with anti-HA antibody (top) and synphilin-1 with anti-myc antibody (middle). The purity of cytosolic and mitochondrial fractions was examined using anti-lactate dehydrogenase (LDH) and anti-voltage-dependent anion channel (VDAC) antibodies, respectively. The percent of uncleaved PINK1 relative to total PINK1 levels in the mitochondrial fractions are shown at the bottom of the figure. (**D**) SH-SY5Y cells were transfected with myc-synphilin-1. Lysates were processed into cytosolic and mitochondrial fractions and analyzed by western blot. Endogenous PINK1 was detected with anti-PINK1 antibody (first panel) and synphilin-1 with anti-myc antibody (second panel). The purity of mitochondrial fractions was examined using anti-LDH and anti-HSP60 antibodies. The percent of endogenous uncleaved PINK1 relative to total PINK1 levels in the mitochondrial fractions are shown at the bottom of the figure. (**E**) SH-SY5Y cells were transfected with myc-synphilin-1 and PINK1-HA (wild-type or KD). When indicated, cells were treated with 1 μM antimycin A and 1 μM oligomycin A for 4 h. Cells lysates were run on a PhosTag gel and levels of phosphorylated synphilin-1 and PINK1 were detected using anti-myc and anti-HA antibodies, respectively. Experiments are representative of four (A) and three (C–E) independent experiments. Values represent the average ± S.E.M. of four experiments (B). *, ** and ***Different from control at $P < 0.05$, $P = 0.01$ and $P = 0.001$, respectively (Student's *t*-test). Scale bar, 25 μm.

mitochondria were highly ubiquitinated in the presence of synphilin-1 and PINK1 (Fig. 8D). In agreement with its dominant negative effects on endogenous SIAH-1 in previous studies (14), SIAH-1 DN inhibited the mitochondrial ubiquitination by synphilin-1 and PINK1 (Fig. 8D). As control, we found that the interaction of synphilin-1 with SIAH-1 DN was similar to that observed with SIAH-1 wild-type (Fig. 8E).

We investigated the role that SIAH plays in mitophagy by using the synphilin-1 VP mutant and SIAH-1 DN. Co-expression of PINK1 and the synphilin-1 VP mutant, a double point mutant (V79N,P81N) that does not bind SIAH-1 (14), failed to promote ubiquitination of mitochondrial proteins (Fig. 8D). Although synphilin-1 VP mutant translocated to the mitochondria similarly than wild-type synphilin-1 (Fig. 8F), it did not support mitophagy (Fig. 8G). Moreover, the catalytically inactive SIAH-1 DN did not interfere with synphilin-1 translocation (Fig. 8F) but prevented mitophagy promoted by synphilin-1 and PINK1 (Fig. 8G). In agreement with the lack of mitophagy in the absence of active SIAH-1, both synphilin-1 VP mutant and SIAH-1 DN decreased the formation of Lamp1 large puncta close to the mitochondria by PINK1–synphilin-1 (Fig. 8H). Knockdown of endogenous SIAH-1 (approximately 90%) inhibited the mitophagy promoted by PINK1 and synphilin-1, confirming that endogenous SIAH is required for the pathway (Fig. 8I and J).

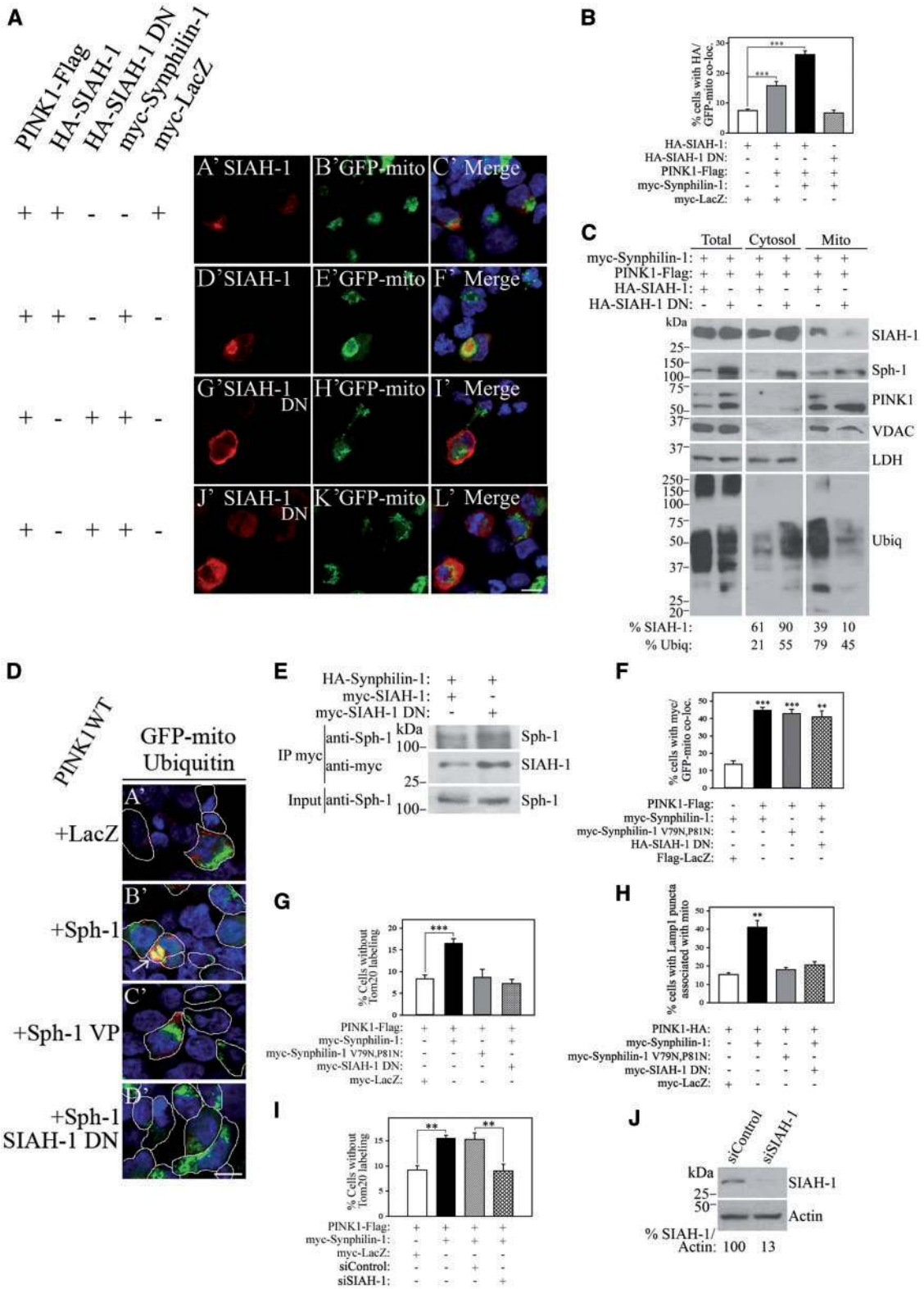

Figure 8. SIAH-1 ubiquitinates mitochondria and is required for PINK1–synphilin-1-mediated mitophagy. (**A**) SH-SY5Y cells were transfected with PINK1-Flag, HA-SIAH-1 (wild-type or SIAH-1 DN; C55A, H59A, C72S) and green fluorescent protein-mito (GFP-mito), in the presence of myc-synphilin-1 or myc-LacZ. Cells were processed for immunocytochemistry using anti-HA, and co-localization of SIAH-1 with GFP-mito was determined by confocal microscopy. (**B**) SH-SY5Y cells were transfected and analyzed as in (A). The graph represents the percentage of HA-SIAH-1 co-localization with mitochondria (GFP-mito). (**C**) SH-SY5Y cells were transfected with PINK1-Flag, myc-synphilin-1, in the presence of HA-SIAH-1 wild-type or SIAH-1 DN. Lysates were fractionated into cytosolic and mitochondrial fractions and were analyzed by western blotting. SIAH-1, synphilin-1 and PINK1 were detected using anti-HA (first panel), anti-myc (second panel) and anti-PINK1 antibodies (third panel), respectively. The extent of mitochondrial ubiquitination was determined using anti-ubiquitin antibody (sixth panel). The purity of cytosolic and mitochondrial fractions

We also investigated the ability of synphilin-1 to translocate and promote mitophagy in the presence of PINK1 disease mutants. We found that the translocation of synphilin-1 to the mitochondria was decreased by at least 50% in the presence of PINK1 disease mutants G309D, A168P and L347P compared to wild-type PINK1 (Fig. 9A and B). Likewise, the ability of synphilin-1 to increase PINK1-dependent mitophagy was inhibited by the disease mutants (Fig. 9C). Purified mitochondrial fractions had significantly less ubiquitination in the presence of synphilin-1 and PINK1 disease mutants (Fig. 9B, bottom). No mitochondrial protein ubiquitination was observed by immunocytochemistry in the presence of synphilin-1 and PINK1 disease mutants (Fig. 9D). Nevertheless, the interaction of synphilin-1 with PINK1 disease mutants was the same as that with PINK1 wild-type when assayed in the absence of intact mitochondria using a detergent-solubilized fraction (Fig. 9E). The data suggest that the lack of synphilin-1 mitochondrial translocation by PINK1 mutants could be due to other factors, such as inability of synphilin-1 to bind PINK1 mutants specifically at the mitochondrial membrane.

PINK1 wild-type or disease mutants did not phosphorylate synphilin-1 (Figs 7E and 9F). Synphilin-1 also did not affect the phosphorylation of ubiquitin by PINK1 wild-type under depolarization conditions (Fig. 9G and H) (27–29). Therefore, although synphilin-1 translocation and mitophagy were disrupted by PINK1 disease mutants, the PINK1–synphilin-1 pathway is independent of PINK1 kinase activity.

Discussion

In the present study, we demonstrated that the PINK1–synphilin-1–SIAH-1 complex promotes mitophagy in the absence of parkin. We showed that synphilin-1 interacts with PINK1 *in vitro* and in cells. PINK1 recruits synphilin-1 to the mitochondria, which leads to mitochondrial depolarization and stabilization of uncleaved PINK1 at the organelle. In turn, synphilin-1 recruits SIAH-1, which ubiquitinates mitochondrial proteins, leading to LC3 recruitment and delivery to lysosomes for mitophagy. PINK1 disease mutants do not engage synphilin-1 in mitophagy, suggesting that decreased activity of the PINK1–synphilin-1–SIAH-1 pathway at the mitochondria could play a role in PD.

We found that synphilin-1 specifically co-immunoprecipitates with PINK1 from brain tissues. Nevertheless, the amount of synphilin-1 that co-immunoprecipitates with PINK1 is smaller than the amount of synphilin-1 present in the brain mitochondria. The reason for this difference is not clear, but it could be related to the fact that the co-immunoprecipitation experiments were done in the presence of harsh detergents while the mitochondria were prepared in the absence of detergents. We also found that PINK1 interacts with synphilin-1 ankyrin-like repeats (9,41), especially with the repeats spanning from amino acids 350 to 549. This preferential interaction is likely related to differences in the binding affinities because the expression of the different constructs was similar.

Although cleaved PINK1 retro-translocates to the cytosol (42), it is also retained at the outer membrane mitochondria, albeit in a more loosely way than uncleaved PINK1 (43–45). Synphilin-1 interacts with both full length and cleaved PINK1 in cells, but there is an apparent selective interaction of synphilin-1 with cleaved PINK1 in the brain. This is likely due to the peculiarities of the anti-PINK1 antibody that we developed, which detects cleaved PINK1 better than the full length counterpart. The scarcity of good antibodies against endogenous PINK1 (45) prevented us to obtain a stronger signal of the uncleaved PINK1 in the brain. The interaction of synphilin-1 with full length and cleaved PINK1 and the depolarization-independent translocation of synphilin-1 to the mitochondria suggest a novel mechanism promoting mitophagy.

Mitophagy promoted by PINK1–synphilin-1–SIAH-1 is supported by several findings. First, PINK1–synphilin-1 decreases the amount of mitochondrial proteins, such as the outer membrane protein Tom20 and the matrix protein HSP60. In addition, PINK1–synphilin-1–SIAH-1 recruits the autophagosome marker LC3 and the lysosome marker Lamp1 to the mitochondria, indicating that once the pathway is activated, mitochondria are processed through autophagy (46). Moreover, degradation of mitochondria by PINK1–synphilin-1 is prevented by autophagy and lysosome inhibitors, as well as by knockdown of the autophagy-related protein Atg5.

Parkin expression or knockdown has no effect on synphilin-1 recruitment to the mitochondria or PINK1–synphilin-1–SIAH-1-mediated mitophagy. Furthermore, we found that the PINK1–synphilin-1–SIAH-1 pathway is also present in HeLa cells that are devoid of parkin (47). These findings suggest that parkin does not play a role in this pathway. The presence of alternative mitophagy pathways has been suggested for Drp1 and Ambra1 (34,36). More recently, PINK1 was shown to promote mitophagy in the absence of parkin via ubiquitin phosphorylation although this pathway is amplified by parkin (48). To the best of our knowledge, synphilin-1-dependent mitophagy is the first PINK1-dependent pathway shown to be unaffected by parkin.

was examined using anti-lactate dehydrogenase (LDH) and anti-voltage-dependent anion channel (VDAC) antibodies, respectively. The percent of SIAH-1 and ubiquitin in cytosolic and mitochondrial fractions relative to their total protein levels are shown at the bottom of the figure. (**D**) SH-SY5Y cells were transfected with GFP-mito, ubiquitin and PINK1-HA, in the presence of myc-synphilin-1 (wild-type or V79N,P81N), myc-SIAH-1 DN or myc-LacZ. Cells were processed for immunocytochemistry using anti-ubiquitin, and co-localization of ubiquitin with GFP-mito was determined by confocal microscopy. Transfected cells are outlined to enable proper visualization, and arrow points to cell containing ubiquitinated mitochondria. (**E**) SH-SY5Y cells were co-transfected with HA-synphilin-1, in the presence of myc-SIAH-1 (wild-type or DN). myc-SIAH-1 were immunoprecipitated using anti-myc antibody (middle), and co-immunoprecipitation of HA-synphilin-1 was detected with anti-synphilin-1 antibody (top). Input levels of HA-synphilin-1 were determined using anti-synphilin-1 antibody (bottom). (**F**) SH-SY5Y cells were transfected with GFP-mito, myc-synphilin-1 (wild-type or V79N,P81N), in the presence of PINK1-Flag, HA-SIAH-1 DN or Flag-LacZ. Cells were processed for immunocytochemistry using anti-myc antibody, and the localization of synphilin-1 at the mitochondria was determined by confocal microscopy. The graph represents the percentage of transfected cells where synphilin-1 co-localizes with GFP-mito. (**G**) SH-SY5Y cells were transfected with PINK1-Flag and GFP, in the presence of myc-synphilin-1 (wild-type or V79N,P81N), myc-SIAH-1 DN or myc-LacZ. Cells were processed for immunocytochemistry using anti-Tom20 antibody, and the presence of Tom20 in GFP-positive cells was determined by confocal microscopy. The graph represents the percentage of transfected cells without Tom20 labeling. (**H**) SH-SY5Y cells were transfected with GFP-mito, RFP-Lamp1, PINK1-HA and myc-synphilin-1 (wild-type or V79N,P81N), in the presence of myc-SIAH-1 DN or myc-LacZ. The graph represents the percentage of cells that have large RFP-Lamp1 puncta closely associated with mitochondria (GFP-mito). (**I**) SH-SY5Y cells were transfected with PINK1-Flag, myc-synphilin-1 and GFP, in the presence of siRNA control or siRNA to SIAH-1. Cells were processed and analyzed as in (**G**). (**J**) SH-SY5Y cells were transfected with siRNA to SIAH-1 or siRNA control. The levels of SIAH-1 in total cell lysates were detected using anti-SIAH-1 antibody (top). The percentages of SIAH-1 present in cell lysates relative to actin are shown at the bottom of the figure. Experiments are representative of four (A) and three (C–E and J) independent experiments. Values represent the average ± S.E.M. of four (B, F, G and I) or three experiments (H). ** and *** Different from control at $P < 0.01$ and $P = 0.001$, respectively (Student's *t*-test). Scale bar, 25 μm.

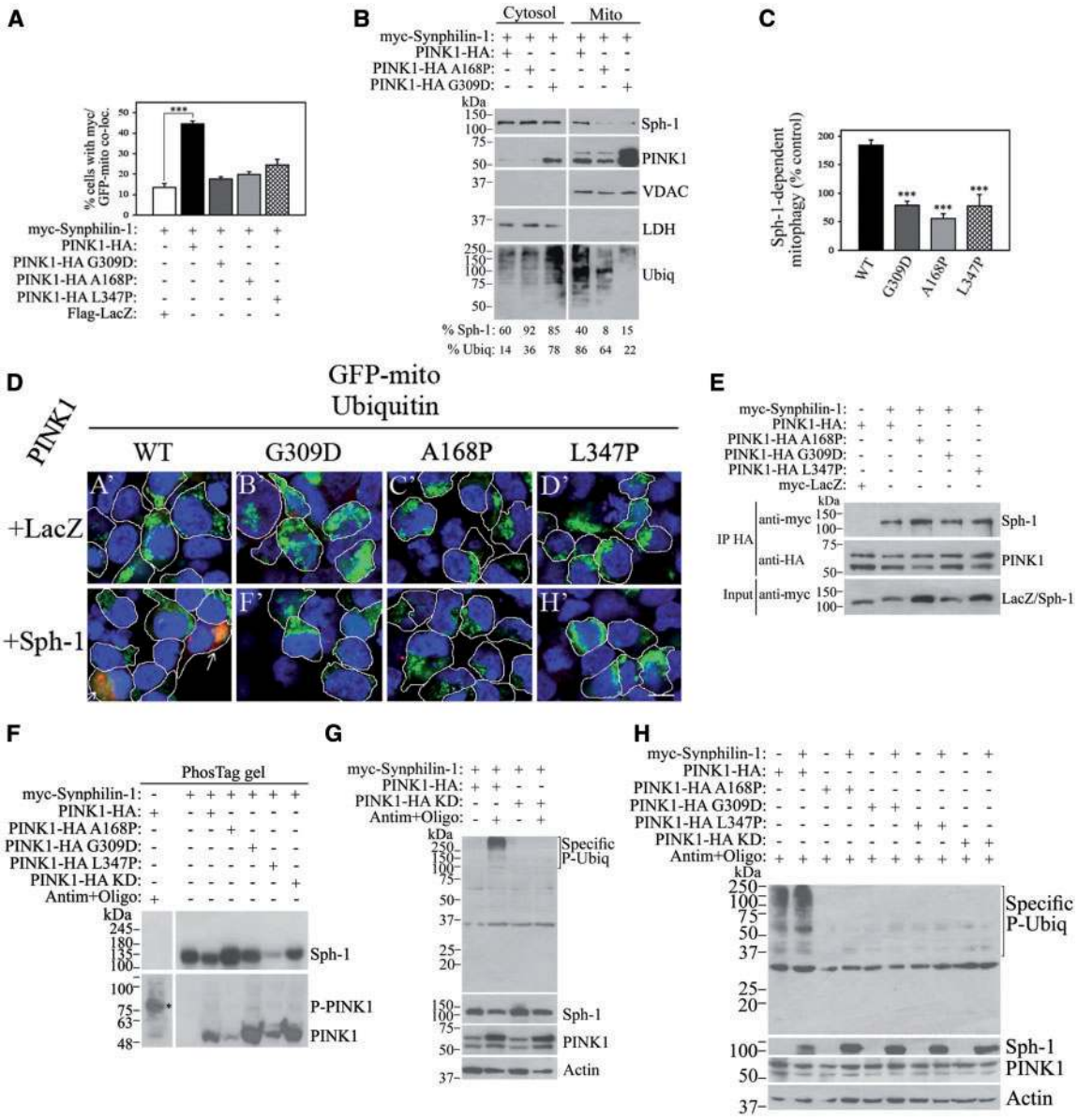

Figure 9. PINK1 disease mutants are defective in the PINK1–synphilin-1 pathway. (**A**) SH-SY5Y cells were transfected with myc-synphilin-1 and green fluorescent protein (GFP), in the presence of PINK1-HA (wild-type, G309D, A168P or L347P) or Flag-LacZ. The presence of Tom20 immunoreactivity in GFP-positive cells was determined by confocal microscopy. The graph represents the percentage of transfected cells without mitochondria (Tom20-negative). (**B**) SH-SY5Y cells were transfected with myc-synphilin-1 and PINK1-HA (wild-type, A168P or G309D). The presence of synphilin-1 and PINK1 in cytosolic and mitochondrial fractions was revealed with anti-myc antibody (first panels) and anti-HA antibody (second panels), respectively. The extent of mitochondrial ubiquitination was determined using anti-ubiquitin antibody (fifth panels). The purity of cytosolic and mitochondrial fractions was examined using anti-lactate dehydrogenase (LDH) and anti-voltage-dependent anion channel (VDAC) antibodies, respectively. The percent of synphilin-1 and ubiquitin in cytosolic and mitochondrial fractions relative to their total protein levels are shown at the bottom of the figure. (**C**) SH-SY5Y cells were transfected with PINK1-HA (wild-type, G309D, A168P or L347P) and GFP, in the presence of myc-synphilin-1 or Flag-LacZ. The presence of Tom20 labeling in GFP-positive cells was determined by confocal microscopy. The graph represents the percentage of mitophagy induced by synphilin-1, compared to LacZ control, and in the presence of PINK1 wild-type or PINK1 disease mutants. (**D**) SH-SY5Y cells were transfected with GFP-mito, ubiquitin and PINK1-HA (wild-type, G309D, A168P or L347P), in the presence of myc-synphilin-1 or myc-LacZ. Cells were processed for immunocytochemistry using anti-ubiquitin, and co-localization of ubiquitin with GFP-mito was determined by confocal microscopy. Transfected cells are outlined and arrows show the co-localization of ubiquitin with GFP-mito in the presence of synphilin-1 and PINK1 wild-type, which is absent with disease mutants. (**E**) SH-SY5Y cells were transfected with PINK1-HA (wild-type or disease mutants) in the presence of myc-synphilin-1 or myc-LacZ. PINK1-HA was immunoprecipitated using anti-HA antibody (middle), and co-immunoprecipitation was detected with anti-myc antibody (top). Input levels of myc-synphilin-1 and myc-LacZ were determined using anti-myc antibody (bottom). (**F**) SH-SY5Y cells were transfected with myc-synphilin-1 in the presence of PINK1-HA (wild-type, disease mutants or KD). When indicated, cells were treated with 1 μM antimycin A and 1 μM oligomycin A for 4 h. Levels of phosphorylated synphilin-1 and PINK1 were detected in PhosTag gel with anti-myc and anti-HA antibodies, respectively. (**G**) SH-SY5Y cells were transfected with myc-synphilin-1 and PINK1-HA (wild-type or KD). When indicated, cells were treated with 1 μM antimycin A and 1 μM oligomycin A for 4 h. The levels of ubiquitin phosphorylation were detected using an anti-phospho-ubiquitin antibody (first panel). Levels of synphilin-1 and PINK1 were monitored with anti-myc and anti-HA antibodies, respectively. Loading control was determined with anti-actin antibody. (**H**) SH-SY5Y cells were transfected with PINK1-HA (wild-type, disease mutants or KD) in the absence and in the presence of myc-synphilin-1, and treated with 1 μM antimycin A and 1 μM oligomycin A for 4 h. The levels of ubiquitin phosphorylation were detected as in (G). Experiments are representative of three independent experiments (B and D–H). Values represent the average ± S.E.M. of four experiments (A and C). ***Different from control at $P < 0.001$ (Student's *t*-test). Scale bar, 25 μm.

Our results indicate that PINK1–synphilin-1–SIAH-1 pathway does not depend on PINK1 kinase activity because both the translocation of synphilin-1 and the mitophagy by catalytically inactive PINK1 (KD) are comparable to that observed with the wild-type protein. Synphilin-1 is not phosphorylated by PINK1, even under depolarization conditions, suggesting that phosphorylation does not act as a signal for synphilin-1 translocation to the mitochondria. Therefore, the ability of PINK1 to recruit synphilin-1 to the mitochondria relies on its direct interaction with synphilin-1 at the mitochondrial membrane. This represents an important aspect that distinguishes the PINK1–synphilin-1 pathway from PINK1–parkin-mediated mitophagy. Furthermore, our observations indicate that synphilin-1 does not alter the levels of phosphoubiquitin in the presence of PINK1 and mitochondrial depolarization. Therefore, synphilin-1 does not interfere with PINK1–parkin pathway, where the phosphorylation of ubiquitin was shown to be instrumental (27–29). The finding that synphilin-1 promotes mitochondrial depolarization in the presence of PINK1, and that synphilin-1 increases uncleaved PINK1 at the mitochondria confirms the significance of PINK1-synphilin-1 pathway. Nevertheless, further studies are necessary to fully understand the mechanism of depolarization promoted by synphilin-1.

In our study, we demonstrated that PINK1–synphilin-1 mitophagy occurs through the recruitment of endogenous SIAH-1 and the ubiquitination it causes to the organelle. SIAH-1 is an ubiquitin-ligase for both synphilin-1 and α-synuclein (14,15,49,50) and some mitochondrial proteins (51,52). In contrast to parkin (26), SIAH-1 does not promote a global degradation of outer mitochondrial membrane proteins prior to mitophagy because proteasome inhibitors do not inhibit PINK1–synphilin-1 mitophagy. Therefore, ubiquitination by SIAH-1 appears to directly recruit LC3 for autophagosome formation.

Synphilin-1 has been implicated in the regulation of autophagy (53). Transgenic mice overexpressing synphilin-1 display higher levels of autophagy markers and less α-synuclein accumulation at the preclinical stage (10). Synphilin-1 promotes the autophagic clearance of α-synuclein inclusions (18), and a region of synphilin-1 containing ankyrin-like repeats could function as a leading sequence to target substrates to the autophagic pathway (19). Our finding that synphilin-1 activates mitophagy highlights its association with different autophagic pathways.

PINK1 disease mutants do not recruit parkin to the mitochondria (21,22). Similarly, we found that PINK1 disease mutants failed to recruit synphilin-1 to the mitochondria or to support mitophagy. These observations support a role of synphilin-1-mediated mitophagy in PD and also confirm the specificity of synphilin-1 recruitment by PINK1. Drugs that enhance synphilin-1-dependent mitophagy may clear dysfunctional mitochondria that are thought to accumulate in PD and may allow more efficient therapeutic approaches for the disease.

Materials and Methods

Cell culture and transfections

Cells were grown in Dulbecco's Modified Eagle Medium (DMEM) containing 10% fetal bovine serum in a 5% carbon dioxide (CO_2) atmosphere. SH-SY5Y or HEK293 cells were transiently transfected with 1 μg of N- and C-terminal-tagged pRK5 plasmids utilizing Lipofectamine 2000 (ThermoFischer Scientific). HeLa cells were transfected with 0.5 μg of N- and C-terminal-tagged pRK5 plasmids utilizing TranslT-LT1 (Mirus Bio LLC) and processed after 36 h. For experiments using siRNAs, cells were transfected with Lipofectamine 2000, as previously described (54), using siPINK1 (5′-GGCAAUUUUUACCCAGAAA-3′), siSIAH-1 (5′-CGCC CAUUCUUCAAUGUCA-3'), siAtg5 (5′-GGCAACCUGACCAGAAA CA-3') or scrambled siRNA control (Ambion). A pool of siRNAs to parkin (5′-UGACCAGAGGAAAGUCACCUGCGAAGGCAATTTTTA CCCAGAAA-3′; 5'-GGAAUGUAAAGAAGCGUACCAUGAA-3'; 5'-UCCAGCUCAAGGAGGUGGUUGCUAA-3') or scrambled siRNA control with high GC duplex were obtained from Invitrogen. A pool of siRNA to synphilin-1 (5′-CAGCGGACCUCCACAAGUA-3′; 5′-GAGCAGCGAACCAGACUUA-3′; 5′-GUAGAAAGCGUAGAGAG UA-3′; 5′-UCAGUCACAUCACUCAAGA-3′) or scrambled siRNA control were obtained from Dharmacon.

Antibody generation

For the anti-PINK1 antibody, rabbits were immunized with amino acids 156–509 of PINK1 fused to GST. Immune serum was passed through a GST-sepharose 4B column to remove anti-GST antibodies. Precleared serum was incubated for 16 h with GST-PINK1 (156–509) immobilized on polyvinylidene fluoride strips. Strips were washed with 20 mM Tris pH 7.4 and 500 mM sodium chloride (NaCl), and the antibody was eluted from the strips with 100 mM glycine (pH 2.5) and dialyzed against phosphate buffered saline (PBS). Anti-synphilin-1, anti-parkin and anti-SIAH-1 antibodies were generated and purified, as previously described (9,14,55).

Western blot analysis

Samples were homogenized as previously described (14). Blots were probed with the following antibodies: mouse anti-hemagglutinin (HA) (Covance, MMS-101), mouse anti-actin (MP Biomedicals, 691001), rabbit anti-myc, rabbit anti-HA, rabbit anti-lactate dehydrogenase, rabbit anti-Tom20, mouse anti-HSP60, mouse anti-ubiquitin, rabbit anti-parkin (Santa Cruz, sc-789, sc-805, sc-33781, sc-11415, sc-376261, sc-8017, sc-30130), rabbit anti-voltage-dependent anion channel (Cell Signaling, 4866S), mouse anti-myc (Sigma, M4439), rabbit anti-Flag (Sigma, F7425) and rabbit anti-phopho-ubiquitin (Boston Biochem A-110). Quantification of enhanced chemiluminescence reactions was performed according to ImageMaster analysis (GE Healthcare Life Sciences, Pittsburgh, PA, USA).

Co-immunoprecipitation assays

For co-immunoprecipitation of synphilin-1 with PINK1, transfected cells were lysed in buffer containing 50 mM Tris (pH 7.4), 140 mM NaCl, 1% Triton X-100, 0.1% sodium dodecyl sulfate (SDS), 30 μM MG132, and a protease inhibitor cocktail (Complete, Roche). Cell extracts were clarified by centrifugation at 13,000*g* for 5 min and incubated for 4 h with anti-HA coupled to protein G beads (Sigma) (14). Immunoprecipitates were washed with lysis buffer containing 500 mM NaCl and detected by western blot analysis. For endogenous co-immunoprecipitation assays, total rat brains were homogenized in the same buffer as above containing 50 mM Tris (pH 7.4), 140 mM NaCl, 1% Triton X-100, 0.1% SDS, 30 μM MG132 and a protease inhibitor cocktail. Brain homogenates were clarified by centrifugation at 13,000*g* for 5 min. The antibody to PINK1 was coupled to protein G beads (14) and incubated for 4 h with brain homogenates (2 mg/ml). Immunoprecipitates were washed with lysis buffer and detected by western blot analysis using an anti-synphilin-1 antibody.

In vivo phosphorylation experiments

After overnight serum starvation in phosphate-free medium, transfected SH-SY5Y cells were incubated for 4 h at 37°C with complete medium. Cells in complete medium were treated with 1 μM oligomycin and 1 μM antimycin A when indicated. Cells were harvested and lysed in buffer containing 50 mM Tris-HCl (pH 7.4), 140 mM NaCl, 1% Triton X-100, 0.1% SDS, phosSTOP (Roche), 30 μM MG132 and protease inhibitor cocktail (Complete, Roche). Lysates were run on 7.5% PhosTag gel (Wako) or 12% PAGE-SDS and detected by western blot analysis.

Mitochondrial preparation

Mitochondria were isolated using a discontinuous Percoll gradient, as previously described (55). Briefly, brain tissues and cells were disrupted using a glass homogenizer in buffer containing 250 mM sucrose, 20 mM Hepes, 3 mM EDTA, 20 mM sodium fluoride, 2 mM sodium orthovanadate, 10 mM inorganic pyrophosphate, 20 mM β-glycerol phosphate, 30 μM MG132, and a protease inhibitor cocktail (Complete, Roche). The washed mitochondrial pellet was resuspended in 15% Percoll in cold homogenizing buffer, layered onto a discontinuous Percoll gradient of 23% over 40%, and then centrifuged for 20 min at 73,000*g* at 4 °C. The interface band between the 23% and 40% Percoll layers was collected and washed twice in cold homogenizing buffer. The mitochondrial pellet was suspended in homogenizing buffer and analyzed by western blot analysis. The percent of synphilin-1, PINK1, SIAH-1 and ubiquitin proteins present in cytosolic and mitochondrial fractions relative to their total protein levels were obtained by ImageMaster analysis and are shown at the bottom of each experiment.

Immunocytochemistry assays

SH-SY5Y cells were fixed in 4% paraformaldehyde for 15 min and blocked in PBS containing 0.2% Triton X-100 and 5% normal goat serum. The cells were labeled with anti-HA, anti-myc, and anti-Flag antibodies, as previously described (14). Immunolabeling was detected using FITC- and Cy^3-labeled secondary antibodies (Jackson Laboratories).

The mitochondrial co-localization experiments in SH-SY5Y cells were performed by co-transfecting GFP-mito (Clontech) (55). The co-localization of synphilin-1 with GFP-mito was determined by processing cells after 36 h of transfection and followed by confocal microscopy analysis. Samples were examined under a Zeiss LSM 700 confocal microscope (Zeiss, Oberkochen, Germany), and optical sections were obtained under a 63× immersion objective at a definition of 1024 × 1024 pixels with the pinhole diameter adjusted to 1 μm. All sections were acquired using the same laser parameters and image magnification. ZEN software (Zeiss) was used to determine the Manders's co-localization coefficient (56). Cells were counted as positive for synphilin-1 and GFP-mito co-localization when the Manders's coefficient of selected areas within the cells were at least 0.5. Approximately 200 cells were examined for each condition in every independent experiment, and data are representative of at least three independent experiments.

For mitochondrial LC3 and Lamp1 co-localization experiments, cells were co-transfected with GFP-mito and RFP-LC3 or RFP-Lamp1 (Addgene), respectively. The association of RFP-LC3 and RFP-Lamp1 large puncta with GFP-mito was determined by processing cells after 36 h of transfection and followed by confocal microscopy analysis (Zeiss LSM 700). Approximately, 200 cells were examined for each condition in every independent experiment. ZEN software was used to visualize and score cells that had large LC3 and Lamp1 puncta in contiguity with GFP-mito, as previously described (36).

For mitophagy experiments in SH-SY5Y and HeLa cells, a small amount of GFP was co-transfected to visualize transfected cells, and mitochondrial presence was determined by staining the endogenous outer mitochondrial membrane protein Tom20 and the matrix mitochondrial protein HSP60 with anti-Tom20 and anti-HSP60 antibodies, respectively (26,55). The percentage of cells lacking mitochondria was determined by processing cells after 36 h of transfection and followed by confocal microscopy analysis (Zeiss LSM 700). For this purpose, 1 μm sections in three different focal planes were acquired for each field. All sections were acquired using the same laser parameters and image magnification. Transfected cells (GFP-positive cells) were scored for mitochondrial presence or absence (Tom20 or HSP60) by analyzing sections from all three focal planes taken for each field, in order to avoid overlooking any mitochondria possibly present in the cells. The images shown represent the best focal plane of a chosen field. Approximately 200 cells were examined for each condition in every independent experiment, and data are representative of at least three independent experiments. The statistics for all confocal analyses mentioned were calculated using paired two-tailed Student's *t*-test.

Live mitochondrial polarization analysis

Mitochondrial membrane potential ($\Delta\Psi_m$) was determined by JC-1 (5,5′,6,6′-tetrachloro-1,1′,3,3′-tetraethylbenzimidazolocarbocyanine iodide) (ThermoFischer Scientific) staining (57). Cells were incubated for 30 min at 37 °C in 5% CO_2 in the presence of 2.5 μg/ml JC-1. Live cell images were acquired using Zeiss LSM 510 Meta Laser Scanning Confocal System (excitation wavelength 488 nm, emission I at 530 ± 15 nm and emission II at 590 ± 20 nm) (Zeiss, Oberkochen, Germany) with 63/1.4× oil objective at a definition of 1024 × 1024 pixels and a pinhole diameter of 3 μm. Red fluorescence indicates JC-1 aggregates formed in cells with normal △ψm, whereas green fluorescence indicates JC-1 monomers in cells with low △ψm. Transfection with blue fluorescent protein (BFP) alone or BFP with 10 μM CCCP (added 30 min before JC-1 incubation) were used as controls for polarized and depolarized mitochondria, respectively.

Acknowledgements

Authors thank Edward A. Fon for providing HeLa cells. We thank former laboratory students Yafit Bez and Sleman Bisharat for their technical help. Authors thank Edith Suss-Toby, Melia Gurewitz and Maya Holdengreber for their help with microscopy and imaging analyses.

Conflict of Interest statement. None declared.

Funding

Israel Academy of Sciences, Teva Pharmaceutical Industries LTD, Rappaport Family Institute for Research in the Medical Sciences, The Allen and Jewel Prince Center for Neurodegenerative Disorders of the Brain, The University of Michigan-Israel Partnership for Research, Bea and Selman Hollander RF in Neurodegenerative Diseases, Rochlin Foundation Fund for Neurodegenerative Disease Research,

Consolidated Anti-Aging Foundation and the Technion Research funds (S.E.).

References

1. Martin, I., Dawson, V.L. and Dawson, T.M. (2011) Recent advances in the genetics of Parkinson's disease. *Annu. Rev. Genomics Hum. Genet.*, **12**, 301–325.
2. Goedert, M., Spillantini, M.G., Del Tredici, K. and Braak, H. (2013) 100 years of Lewy pathology. *Nat. Rev. Neurol*, **9**, 13–24.
3. Hardy, J. (2010) Genetic analysis of pathways to Parkinson disease. *Neuron*, **68**, 201–206.
4. Spillantini, M.G., Schmidt, M.L., Lee, V.M., Trojanowski, J.Q., Jakes, R. and Goedert, M. (1997) Alpha-synuclein in Lewy bodies. *Nature*, **388**, 839–840.
5. Kitada, T., Asakawa, S., Hattori, N., Matsumine, H., Yamamura, Y., Minoshima, S., Yokochi, M., Mizuno, Y. and Shimizu, N. (1998) Mutations in the parkin gene cause autosomal recessive juvenile parkinsonism. *Nature*, **392**, 605–608.
6. Valente, E.M., Abou-Sleiman, P.M., Caputo, V., Muqit, M.M., Harvey, K., Gispert, S., Ali, Z., Del Turco, D., Bentivoglio, A.R., Healy, D.G., *et al.* (2004) Hereditary early-onset Parkinson's disease caused by mutations in PINK1. *Science*, **304**, 1158–1160.
7. Scarffe, L.A., Stevens, D.A., Dawson, V.L. and Dawson, T.M. (2014) Parkin and PINK1: much more than mitophagy. *Trends Neurosci.*, **37**, 315–324.
8. Grenier, K., McLelland, G.L. and Fon, E.A. (2013) Parkin- and PINK1-Dependent Mitophagy in Neurons: Will the Real Pathway Please Stand Up? *Front. Neurol.*, **4**, 100.
9. Engelender, S., Kaminsky, Z., Guo, X., Sharp, A.H., Amaravi, R.K., Kleiderlein, J.J., Margolis, R.L., Troncoso, J.C., Lanahan, A.A., Worley, P.F., *et al.* (1999) Synphilin-1 associates with alpha-synuclein and promotes the formation of cytosolic inclusions. *Nat. Genet*, **22**, 110–114.
10. Smith, W.W., Liu, Z., Liang, Y., Masuda, N., Swing, D.A., Jenkins, N.A., Copeland, N.G., Troncoso, J.C., Pletnikov, M., Dawson, T.M., *et al.* (2010) Synphilin-1 attenuates neuronal degeneration in the A53T alpha-synuclein transgenic mouse model. *Hum. Mol. Genet.*, **19**, 2087–2098.
11. Casadei, N., Pohler, A.M., Tomas-Zapico, C., Torres-Peraza, J., Schwedhelm, I., Witz, A., Zamolo, I., De Heer, R., Spruijt, B., Noldus, L.P., *et al.* (2014) Overexpression of synphilin-1 promotes clearance of soluble and misfolded alpha-synuclein without restoring the motor phenotype in aged A30P transgenic mice. *Hum. Mol. Genet.*, **23**, 767–781.
12. Wakabayashi, K., Engelender, S., Yoshimoto, M., Tsuji, S., Ross, C.A. and Takahashi, H. (2000) Synphilin-1 is present in Lewy bodies in Parkinson's disease. *Ann. Neurol.*, **47**, 521–523.
13. Chung, K.K., Zhang, Y., Lim, K.L., Tanaka, Y., Huang, H., Gao, J., Ross, C.A., Dawson, V.L. and Dawson, T.M. (2001) Parkin ubiquitinates the alpha-synuclein-interacting protein, synphilin-1: implications for Lewy-body formation in Parkinson disease. *Nat. Med.*, **7**, 1144–1150.
14. Liani, E., Eyal, A., Avraham, E., Shemer, R., Szargel, R., Berg, D., Bornemann, A., Riess, O., Ross, C.A., Rott, R., *et al.* (2004) Ubiquitylation of synphilin-1 and alpha-synuclein by SIAH and its presence in cellular inclusions and Lewy bodies imply a role in Parkinson's disease. *Proc. Natl. Acad. Sci. U. S. A.*, **101**, 5500–5505.
15. Nagano, Y., Yamashita, H., Takahashi, T., Kishida, S., Nakamura, T., Iseki, E., Hattori, N., Mizuno, Y., Kikuchi, A. and Matsumoto, M. (2003) Siah-1 facilitates ubiquitination and degradation of synphilin-1. *J. Biol. Chem.*, **278**, 51504–51514.
16. Feng, Y., He, D., Yao, Z. and Klionsky, D.J. (2014) The machinery of macroautophagy. *Cell Res.*, **24**, 24–41.
17. Sanchez-Danes, A., Richaud-Patin, Y., Carballo-Carbajal, I., Jimenez-Delgado, S., Caig, C., Mora, S., Di Guglielmo, C., Ezquerra, M., Patel, B., Giralt, A., *et al.* (2012) Disease-specific phenotypes in dopamine neurons from human iPS-based models of genetic and sporadic Parkinson's disease. *EMBO Mol. Med*, **4**, 380–395.
18. Wong, E.S., Tan, J.M., Soong, W.E., Hussein, K., Nukina, N., Dawson, V.L., Dawson, T.M., Cuervo, A.M. and Lim, K.L. (2008) Autophagy-mediated clearance of aggresomes is not a universal phenomenon. *Hum. Mol. Genet.*, **17**, 2570–2582.
19. Wong, E., Bejarano, E., Rakshit, M., Lee, K., Hanson, H.H., Zaarur, N., Phillips, G.R., Sherman, M.Y. and Cuervo, A.M. (2012) Molecular determinants of selective clearance of protein inclusions by autophagy. *Nat. Commun.*, **3**, 1240.
20. Narendra, D., Tanaka, A., Suen, D.F. and Youle, R.J. (2008) Parkin is recruited selectively to impaired mitochondria and promotes their autophagy. *J. Cell Biol.*, **183**, 795–803.
21. Vives-Bauza, C., Zhou, C., Huang, Y., Cui, M., de Vries, R.L., Kim, J., May, J., Tocilescu, M.A., Liu, W., Ko, H.S., *et al.* (2010) PINK1-dependent recruitment of Parkin to mitochondria in mitophagy. *Proc. Natl. Acad. Sci. U. S. A.*, **107**, 378–383.
22. Narendra, D.P., Jin, S.M., Tanaka, A., Suen, D.F., Gautier, C.A., Shen, J., Cookson, M.R. and Youle, R.J. (2010) PINK1 is selectively stabilized on impaired mitochondria to activate Parkin. *PLoS Biol.*, **8**, e1000298.
23. Tanaka, A., Cleland, M.M., Xu, S., Narendra, D.P., Suen, D.F., Karbowski, M. and Youle, R.J. (2010) Proteasome and p97 mediate mitophagy and degradation of mitofusins induced by Parkin. *J. Cell Biol.*, **191**, 1367–1380.
24. Matsuda, N., Sato, S., Shiba, K., Okatsu, K., Saisho, K., Gautier, C.A., Sou, Y.S., Saiki, S., Kawajiri, S., Sato, F., *et al.* (2010) PINK1 stabilized by mitochondrial depolarization recruits Parkin to damaged mitochondria and activates latent Parkin for mitophagy. *J. Cell Biol.*, **189**, 211–221.
25. Geisler, S., Holmstrom, K.M., Skujat, D., Fiesel, F.C., Rothfuss, O.C., Kahle, P.J. and Springer, W. (2010) PINK1/Parkin-mediated mitophagy is dependent on VDAC1 and p62/SQSTM1. *Nat. Cell Biol.*, **12**, 119–131.
26. Chan, N.C., Salazar, A.M., Pham, A.H., Sweredoski, M.J., Kolawa, N.J., Graham, R.L., Hess, S. and Chan, D.C. (2011) Broad activation of the ubiquitin-proteasome system by Parkin is critical for mitophagy. *Hum. Mol. Genet.*, **20**, 1726–1737.
27. Kane, L.A., Lazarou, M., Fogel, A.I., Li, Y., Yamano, K., Sarraf, S.A., Banerjee, S. and Youle, R.J. (2014) PINK1 phosphorylates ubiquitin to activate Parkin E3 ubiquitin ligase activity. *J. Cell Biol.*, **205**, 143–153.
28. Kazlauskaite, A., Kondapalli, C., Gourlay, R., Campbell, D.G., Ritorto, M.S., Hofmann, K., Alessi, D.R., Knebel, A., Trost, M. and Muqit, M.M. (2014) Parkin is activated by PINK1-dependent phosphorylation of ubiquitin at Ser65. *Biochem. J.*, **460**, 127–139.
29. Koyano, F., Okatsu, K., Kosako, H., Tamura, Y., Go, E., Kimura, M., Kimura, Y., Tsuchiya, H., Yoshihara, H., Hirokawa, T., *et al.* (2014) Ubiquitin is phosphorylated by PINK1 to activate parkin. *Nature*, **510**, 162–166.
30. Michiorri, S., Gelmetti, V., Giarda, E., Lombardi, F., Romano, F., Marongiu, R., Nerini-Molteni, S., Sale, P., Vago, R., Arena, G., *et al.* (2010) The Parkinson-associated protein PINK1 interacts with Beclin1 and promotes autophagy. *Cell Death Differ.*, **17**, 962–974.

31. Bueler, H. (2009) Impaired mitochondrial dynamics and function in the pathogenesis of Parkinson's disease. *Exp. Neurol*, **218**, 235–246.
32. Zhu, J., Wang, K.Z. and Chu, C.T. (2013) After the banquet: mitochondrial biogenesis, mitophagy, and cell survival. *Autophagy*, **9**, 1663–1676.
33. Wang, K. and Klionsky, D.J. (2011) Mitochondria removal by autophagy. *Autophagy*, **7**, 297–300.
34. Thomas, K.J., McCoy, M.K., Blackinton, J., Beilina, A., van der Brug, M., Sandebring, A., Miller, D., Maric, D., Cedazo-Minguez, A. and Cookson, M.R. (2011) DJ-1 acts in parallel to the PINK1/parkin pathway to control mitochondrial function and autophagy. *Hum. Mol. Genet.*, **20**, 40–50.
35. Van Humbeeck, C., Cornelissen, T., Hofkens, H., Mandemakers, W., Gevaert, K., De Strooper, B. and Vandenberghe, W. (2011) Parkin interacts with Ambra1 to induce mitophagy. *J. Neurosci.*, **31**, 10249–10261.
36. Strappazzon, F., Nazio, F., Corrado, M., Cianfanelli, V., Romagnoli, A., Fimia, G.M., Campello, S., Nardacci, R., Piacentini, M., Campanella, M., *et al.* (2014) AMBRA1 is able to induce mitophagy via LC3 binding, regardless of PARKIN and p62/SQSTM1. *Cell Death Differ.*, **22**, 419–432.
37. Bandopadhyay, R., Kingsbury, A.E., Muqit, M.M., Harvey, K., Reid, A.R., Kilford, L., Engelender, S., Schlossmacher, M.G., Wood, N.W., Latchman, D.S., *et al.* (2005) Synphilin-1 and parkin show overlapping expression patterns in human brain and form aggresomes in response to proteasomal inhibition. *Neurobiol. Dis.*, **20**, 401–411.
38. Ribeiro, C.S., Carneiro, K., Ross, C.A., Menezes, J.R. and Engelender, S. (2002) Synphilin-1 is developmentally localized to synaptic terminals, and its association with synaptic vesicles is modulated by alpha-synuclein. *J. Biol. Chem.*, **277**, 23927–23933.
39. Lim, K.L., Chew, K.C., Tan, J.M., Wang, C., Chung, K.K., Zhang, Y., Tanaka, Y., Smith, W., Engelender, S., Ross, C.A., *et al.* (2005) Parkin mediates nonclassical, proteasomal-independent ubiquitination of synphilin-1: implications for Lewy body formation. *J. Neurosci.*, **25**, 2002–2009.
40. Mizushima, N., Noda, T., Yoshimori, T., Tanaka, Y., Ishii, T., George, M.D., Klionsky, D.J., Ohsumi, M. and Ohsumi, Y. (1998) A protein conjugation system essential for autophagy. *Nature*, **395**, 395–398.
41. Kruger, R. (2004) The role of synphilin-1 in synaptic function and protein degradation. *Cell Tissue Res*, **318**, 195–199.
42. Yamano, K. and Youle, R.J. (2013) PINK1 is degraded through the N-end rule pathway. *Autophagy*, **9**, 1758–1769.
43. Becker, D., Richter, J., Tocilescu, M.A., Przedborski, S. and Voos, W. (2012) Pink1 kinase and its membrane potential (Deltapsi)-dependent cleavage product both localize to outer mitochondrial membrane by unique targeting mode. *J. Biol. Chem.*, **287**, 22969–22987.
44. Fedorowicz, M.A., de Vries-Schneider, R.L., Rub, C., Becker, D., Huang, Y., Zhou, C., Alessi Wolken, D.M., Voos, W., Liu, Y. and Przedborski, S. (2014) Cytosolic cleaved PINK1 represses Parkin translocation to mitochondria and mitophagy. *EMBO Rep.*, **15**, 86–93.
45. Lim, G.G., Chua, D.S., Basil, A.H., Chan, H.Y., Chai, C., Arumugam, T. and Lim, K.L. (2015) Cytosolic PTEN-induced Putative Kinase 1 Is Stabilized by the NF-kappaB Pathway and Promotes Non-selective Mitophagy. *J. Biol. Chem.*, **290**, 16882–16893.
46. Klionsky, D.J., Abdalla, F.C., Abeliovich, H., Abraham, R.T., Acevedo-Arozena, A., Adeli, K., Agholme, L., Agnello, M., Agostinis, P., Aguirre-Ghiso, J.A., *et al.* (2012) Guidelines for the use and interpretation of assays for monitoring autophagy. *Autophagy*, **8**, 445–544.
47. Denison, S.R., Wang, F., Becker, N.A., Schule, B., Kock, N., Phillips, L.A., Klein, C. and Smith, D.I. (2003) Alterations in the common fragile site gene Parkin in ovarian and other cancers. *Oncogene*, **22**, 8370–8378.
48. Lazarou, M., Sliter, D.A., Kane, L.A., Sarraf, S.A., Wang, C., Burman, J.L., Sideris, D.P., Fogel, A.I. and Youle, R.J. (2015) The ubiquitin kinase PINK1 recruits autophagy receptors to induce mitophagy. *Nature*, **524**, 309–314.
49. Rott, R., Szargel, R., Haskin, J., Shani, V., Shainskaya, A., Manov, I., Liani, E., Avraham, E. and Engelender, S. (2008) Monoubiquitylation of alpha-synuclein by seven in absentia homolog (SIAH) promotes its aggregation in dopaminergic cells. *J. Biol. Chem.*, **283**, 3316–3328.
50. Lee, J.T., Wheeler, T.C., Li, L. and Chin, L.S. (2008) Ubiquitination of alpha-synuclein by Siah-1 promotes alpha-synuclein aggregation and apoptotic cell death. *Hum. Mol. Genet.*, **17**, 906–917.
51. Habelhah, H., Laine, A., Erdjument-Bromage, H., Tempst, P., Gershwin, M.E., Bowtell, D.D. and Ronai, Z. (2004) Regulation of 2-oxoglutarate (alpha-ketoglutarate) dehydrogenase stability by the RING finger ubiquitin ligase Siah. *J. Biol. Chem.*, **279**, 53782–53788.
52. Garrison, J.B., Correa, R.G., Gerlic, M., Yip, K.W., Krieg, A., Tamble, C.M., Shi, R., Welsh, K., Duggineni, S., Huang, Z., *et al.* (2011) ARTS and Siah collaborate in a pathway for XIAP degradation. *Mol. Cell*, **41**, 107–116.
53. Li, X., Tamashiro, K.L., Liu, Z., Bello, N.T., Wang, X., Aja, S., Bi, S., Ladenheim, E.E., Ross, C.A., Moran, T.H., *et al.* (2012) A novel obesity model: synphilin-1-induced hyperphagia and obesity in mice. *Int. J. Obes. (Lond)*, **36**, 1215–1221.
54. Avraham, E., Rott, R., Liani, E., Szargel, R. and Engelender, S. (2007) Phosphorylation of Parkin by the Cyclin-dependent Kinase 5 at the Linker Region Modulates Its Ubiquitin-Ligase Activity and Aggregation. *J. Biol. Chem.*, **282**, 12842–12850.
55. Haskin, J., Szargel, R., Shani, V., Mekies, L.N., Rott, R., Lim, G.G., Lim, K.L., Bandopadhyay, R., Wolosker, H. and Engelender, S. (2013) AF-6 is a positive modulator of the PINK1/parkin pathway and is deficient in Parkinson's disease. *Hum. Mol. Genet.*, **22**, 2083–2096.
56. Zinchuk, V., Zinchuk, O. and Okada, T. (2005) Experimental LPS-induced cholestasis alters subcellular distribution and affects colocalization of Mrp2 and Bsep proteins: a quantitative colocalization study. *Microsc. Res. Tech.*, **67**, 65–70.
57. Ben-Shachar, D., Suss-Toby, E. and Robicsek, O. (2015) Analysis of mitochondrial network by imaging: proof of technique in schizophrenia. *Methods Mol. Biol.*, **1265**, 425–439.